Journal of Materials Chemistry C

Triplet Conformation in Chromophore-fused Cyclooctatetraene Dyes

Journal:	*Journal of Materials Chemistry C*
Manuscript ID	TC-ART-06-2023-002151.R2
Article Type:	Paper
Date Submitted by the Author:	03-Aug-2023
Complete List of Authors:	Paul, Sunandita; Tata Institute of Fundamental Research Kitakado, Hidetsugu; Kyoto University, Department of Chemistry, Graduate School of Science Suga, Kensuke; Kyoto University, Department of Chemistry, Graduate School of Science Kotani, Ryota; Kyoto University, Department of Chemistry, Graduate School of Science Dey, Nilanjan; Birla Institute of Technology and Science - Hyderabad Campus, Department of Chemistry; Kyoto University - Yoshida Campus, Matito, Eduard; Donostia International Physics Center, Donostia International Physics Center Venkatramani, Ravindra ; Tata Institute of Fundamental Research, Chemical Sciences; Tata Institute of Fundamental Research Saito, Shohei; Kyoto University, Department of Chemistry, Graduate School of Science Dasgupta, Jyotishman; Tata Institute of Fundamental Research, Department of Chemical Sciences

ARTICLE

Triplet Conformation in Chromophore-fused Cyclooctatetraene Dyes

Sunandita Paul,[a] Hidetsugu Kitakado,[b] Kensuke Suga,[b] Ryota Kotani,[b] Nilanjan Dey[b], Ravindra Venkatramani,[a] Eduard Matito[c], Shohei Saito[b]* and Jyotishman Dasgupta[a]*

Received 00th January 20xx,
Accepted 00th January 20xx

DOI: 10.1039/x0xx00000x

Cyclooctatetraene (COT) has a tub-shaped conformation in its ground non-aromatic state while it is predicted to have a planar aromatic triplet state. However, COT possesses a non-vertical triplet state, and therefore their detection has remained elusive through direct photoexcitation. Recently fluorescent dyes synthesized by fusing COT with anthracene and phenazine "wings" have shown large Stokes shift implying a significant conformational change in their excited singlet manifold. Here using broadband transient absorption spectroscopy supported with electronic structure calculations, we demonstrate that the intersystem crossing occurs in the planar COT conformation in these flapping dyes. We confirm that such a planar conformation in the triplet state does not impart aromaticity to the COT backbone, as previously predicted. Our work therefore provides the basis for the requisite structural design principles that would allow for triplet formation from excited singlet states in COT-based functional molecules.

Introduction

Cyclooctatetraene (COT) is the smallest non-planar annulene with 4nπ electrons that has a "tub" shaped structure in its ground state[1-5]. Temperature-dependent NMR studies and subsequent time-resolved photoelectron spectroscopy measurements indicated a dynamic interconversion between the "tub" shape conformation through a planar anti-aromatic COT transition state[6-11]. Baird rules predict that 4nπ annulene systems can have aromatic stabilization in the lowest triplet excited state by attaining a planar molecular geometry[12-14]. Due to the large aromatic stabilization of the low-lying triplet state, COT has been a popular triplet quencher lending in vivo photostability to covalently functionalized bio-imaging molecular probes[15-19]. While the appearance of COT triplet is commonly discussed through the triplet energy transfer from photoexcited organic dyes, triplet COT is not directly populated via intersystem crossing after vertical excitation[20-24] (Figure 1). Recently, the predicted aromatic planar geometry of COT in the excited state was confirmed through time-resolved IR and ultrafast electron diffraction measurements in a sterically-constrained derivative of COT[25]. Thus, the conformational flexibility of COT both in the ground and excited states can lead to the transient planarization of the backbone. Leveraging the conformational flexibility of the COT ring in the excited state, Saito and co-workers synthesized a series of "flapping" fluorophores by attaching suitable acene chromophores as "wings" symmetrically around the central COT ring[26-28]. Photoexcitation of these dyes by UV light (~365 nm) leads to green fluorescence with high-quantum yield and substantial Stokes shift. It was conjectured that large amplitude movement of the chromophore "wings" driven by the planarization of the COT backbone enabled sensitivity of the emission to solvent viscosity at the nanoscale[26,29]. Recently the phenazine version of the COT dyes were reported with large absorption cross-section in the visible window (>400 nm) and long-term stability in single molecule spectroscopy experiments[30]. Through these set of molecular dyes, it was

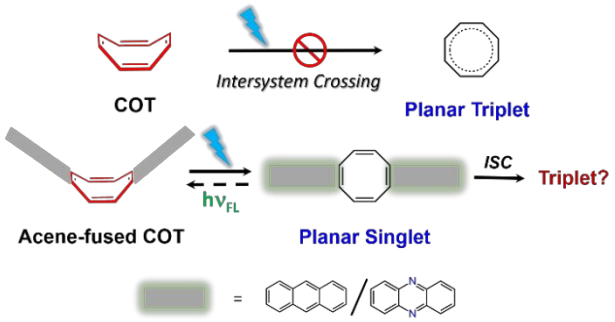

Figure 1. Conceptual representation of possible excited planar states in native COT and acene-fused COT dyes.

[a.] Sunandita Paul, Ravindra Venkatramani and Jyotishman Dasgupta
Tata Institute of Fundamental Research,
Department of Chemical Sciences, Tata Institute of Fundamental Research,
Mumbai 400005, India
Email: dasgupta@tifr.res.in
[b.] Hidetsugu Kitakado, Kensuke Suga, Ryota Kotani, Nilanjan Dey and Shohei Saito
Department of Chemistry, Graduate School of Science, Kyoto University,
Kyoto, Japan
Email: saito.shohei.4c@kyoto-u.ac.jp
[c.] Eduard Matito
Donostia International Physics Center (DIPC),
Manuel Lardizabal Ibilbidea 4, 20018 Donostia, Euskadi, Spain; and
Ikerbasque, Basque Foundation of Science, 48009 Bilbao, Euskadi, Spain

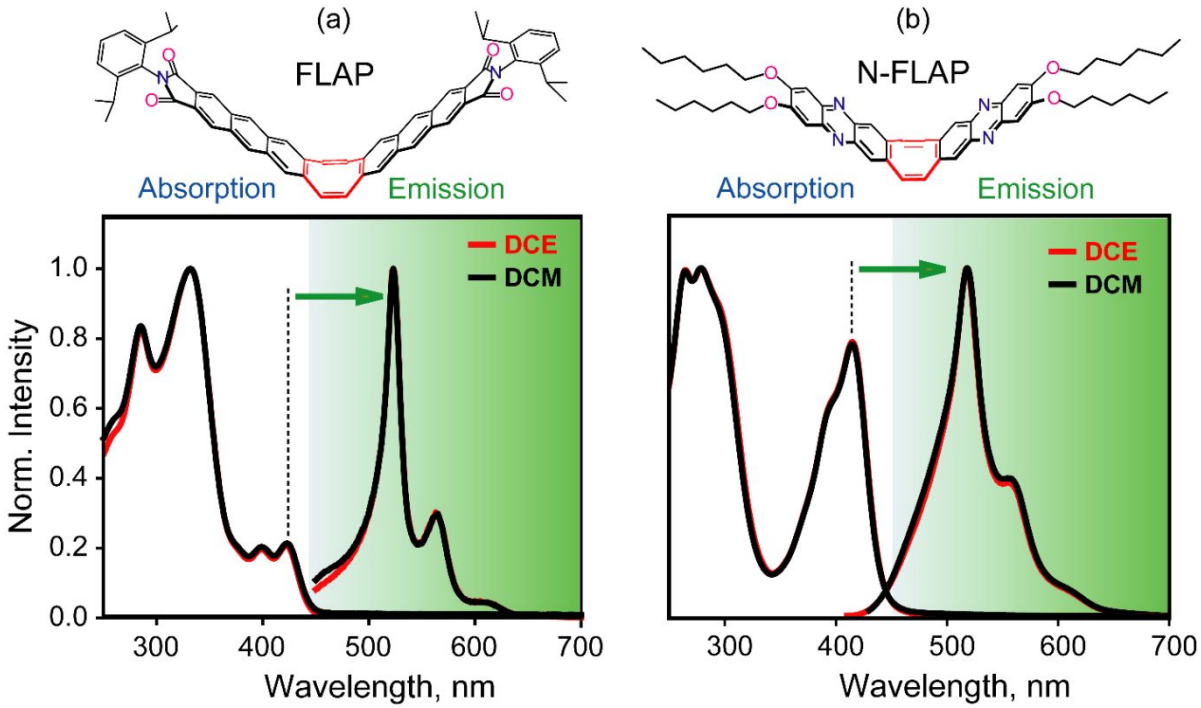

Figure 2. (a) Chemical structure of **FLAP** with normalized absorption and emission (green shaded area) in DCM (black line) and DCE (red line). (b) Chemical structure of **N-FLAP** with normalized absorption and emission (green shaded area) in DCM (black line) and DCE (red line). The green arrow shows the Stokes shift in emission on 400 nm excitation both in (a) and (b).

noted that photoexcitation of the annulated COT derivatives can lead to planarization in the singlet state[31-33].However optical signatures of the putative triplet state in these molecular dyes have been elusive.

Figure 1 represents the predicted structures of COT and COT-based flapping fluorophores in their respective excited states. Due to poor intersystem crossing rates in COT[20,24], the planar triplet state with predicted aromaticity[12] cannot be directly accessed by singlet excitation. Native COT has a non-vertical planar triplet state[20-21,34-35] while it is hypothesized that acene-fused COT dyes could be vertically excited through the chromophoric centres to their respective planar singlet (and triplet) state. Here we probe the excited state evolution of COT-based flapping fluorophores and track the formation of the triplet states using time-resolved absorption spectroscopy. Using timescales spanning from femtoseconds to microseconds, we obtained transient absorption spectra of anthracene (**FLAP**) and the phenazine versions (**N-FLAP**) of the flapping fluorophore as it evolves from the planar singlet state to the triplet state.

Results and Discussion

Characterization of the optical signatures: The synthesis of pure **FLAP** and **N-FLAP** were carried out as reported previously[27,30]. The chemical structures of both **FLAP** and **N-FLAP** (see Figure 2a and Figure 2b) as per the reported crystal structure enunciates the non-planarity of the COT ring in its ground state. To characterize the planarization dynamics, we carried out spectroscopic measurements in both dichloromethane (DCM) with viscosity of η = 0.44 cP at 20 °C and its isopolar yet slightly more viscous analogue 1,2-dichloroethane (DCE; η = 0.84 cP at 20 °C). Figure 2 shows the steady state absorption and emission of **FLAP** and **N-FLAP** in DCM and DCE. Pronounced vibrionic features observed between 375 nm and 450 nm characterize the lowest energy absorption arising from anthracene-centric absorption of **FLAP** (Figure 2a) while these are slightly subdued in the phenazine-centric absorption of **N-FLAP** (Figure 2b). As the control experiments, the monomers of anthraceneimide[36] and phenazine[37] bearing the same substituents have been also studied (Figure S1). In the absence of the fused COT center, only a slight blue shift was observed in their absorption spectra.

We obtained emission spectra in DCM and DCE upon exciting at 400 nm, which represents the chromophore-centric transitions. The emission is structured and highly Stokes shifted in both solvents with maxima at 523 nm for **FLAP** and 518 nm for **N-FLAP**. It should be noted that this large Stokes shift in emission is not present in the corresponding monomer "wing" of both the chromophores (Figure S1). However, there is a low intensity emission band around ~475 nm for both the flapping molecules under the envelope of strong Stokes-shifted emission maxima, which has been assigned as a fluorescence emitted from the slightly relaxed shallow V-shaped geometry in S_1[26]. The large Stokes shift (>3000 cm^{-1}) of the intense emission maxima in both the cases cannot be explained by vibrational cooling of the locally excited (LE) state. In fact, it has been implied previously that the LE state evolves quickly to the emissive state with a high quantum yield. The excitation spectra match well with the absorption

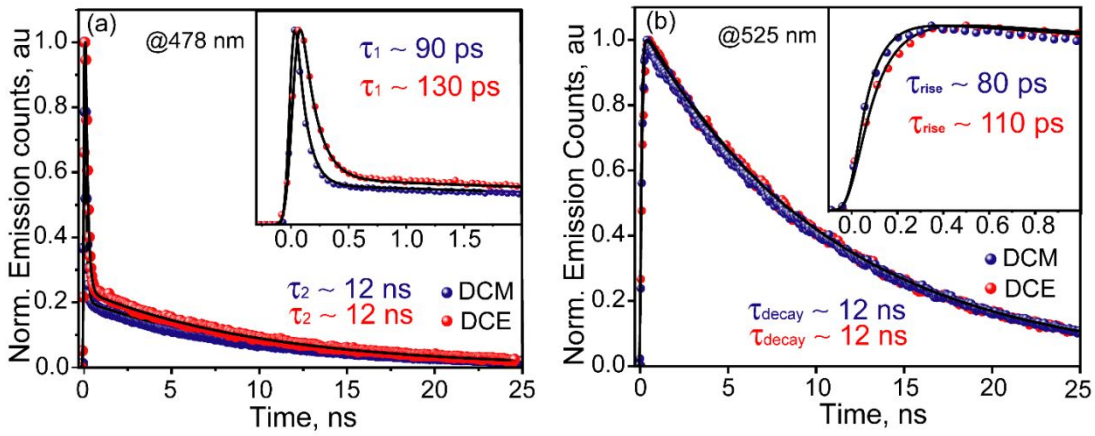

Figure 3. Time-correlated single photon counting measurements: Emission lifetime of **FLAP** in DCM (blue trace) and DCE (red trace) subsequent to 400 nm excitation monitored at (a) 478 nm (b) 525 nm.

spectra, indicating no intermolecular interaction in the ground state in the sample solution (Figure S2).

Fluorescence lifetime and its viscosity dependence: To further check whether the emission centered at 523 nm for **FLAP** and 518 nm for **N-FLAP** arises from a relaxed excited state, viscosity-dependent fluorescence lifetime measurements were carried out using time-correlated single photon counting (TCSPC). The idea was to probe the lifetime of both the slightly relaxed emissive state (~475 nm) bearing the shallow V-shaped geometry and the fully relaxed emissive state (~525 nm) bearing the planarized geometry. Figure 3 shows emission decays of **FLAP** in DCM/DCE at 478 nm and 525 nm respectively. The emission counts monitored at 478 nm decays in a biexponential manner in both the solvents (Figure 3a). The faster component (amplitude 88%) decays with a lifetime of 90 ps in DCM and 130 ps in DCE, respectively. The slower component has similar lifetimes of ~12 ns in both the solvents. The retardation of the decay from the slightly relaxed state in more viscous DCE implies a large amplitude structural change leading to the fully planarized state. Interestingly, the time-resolved emission trace at 525 nm shows a viscosity-dependent rise time which increases from 80 ps in DCM to 110 ps in DCE. The subsequent decay is mono-exponential with ~12 ns lifetime in both the solvents is similar to that observed at 478 nm. Such a viscosity dependent rise of the 525 nm emission which is concomitant with the decay of the 478 nm emission suggests an excited state evolution through a two-state sequential model. Indeed, potential energy scans of the S_1 surface by Saito and co-workers[26,30,38] indicate a conformational planarization of **FLAP**. The 12 ns component observed at 478 nm would be due to the blue tail of the fully relaxed emissive state (max = 523 nm) which overlaps with the blue fluorescence from the slightly relaxed emissive state. The similar scheme is also predicted for **N-FLAP** (see Figure S3),[30] whose emission shows viscosity-sensitivity in both the decay profile at 460 nm (~60 ps in DCM which is slowed down to ~80 ps in DCE) and the rise at 515 nm (~70 ps in DCM which increases to 80 ps in DCE). At both the wavelengths, we observe a ~2.3 ns component indicating the final fluorescence lifetime of the structurally relaxed excited state.

In order to further prove the slower planarization in more viscous solvent mineral oil (with a viscosity of 25 cP) was used to observe the planarization through emission lifetime studies. The steady state emission spectra of both FLAP and N-FLAP (shown in Figure S2 c and d) show an increased intensity in the blue side. The emission lifetimes monitored for FLAP at 475 nm shows an order of magnitude higher lifetime of 1.7 ns and a rise of 2.7 ns in the planarization dynamics as shown by emission decay at 520 nm. The 520 nm emission lifetime shows the planar state to have an 16 ns lifetime which is comparable to that observed in DCM. Similarly for N-FLAP the bent S1 emissive state lifetime is now enhanced to 320 ps (compared to 60 ps in DCM) as seen from the decay at 460 nm and a concomitant rise of 350 ps at 550 nm emission dynamics. The planar state shows a lifetime of 3 ns as compared to 2.3 ns in DCM. Thus we see that in an order of magnitude higher viscous solvent the planarization gets slower by the same order of magnitude confirming the structural change happening.

Femtosecond transient absorption studies in the visible range: To elucidate the faster dynamics and the absorption spectra of excited states, femtosecond (fs) to nanosecond (ns) transient absorption was measured. Figure 4a shows the transient absorption spectra of **FLAP** in DCM in the visible range of 440 nm to 800 nm under inert conditions after a 400 nm short pulse excitation. The TA spectrum was deconvoluted to give evolution associated spectra in Figure 4b. After excitation by the pump laser, we observe a broad absorption with a maximum at 525 nm (black trace with ~15 ps lifetime), which evolves with time initially to a blue-shifted feature at 500 nm (red trace with ~70 ps lifetime), and then to a narrower absorption profile at 490 nm with enhanced intensity (green trace with > 2ns lifetime in Figure 4b). The 70 ps lifetime of the intermediate state matches with the ~80 ps lifetime of the slightly relaxed emissive state (assigned with a

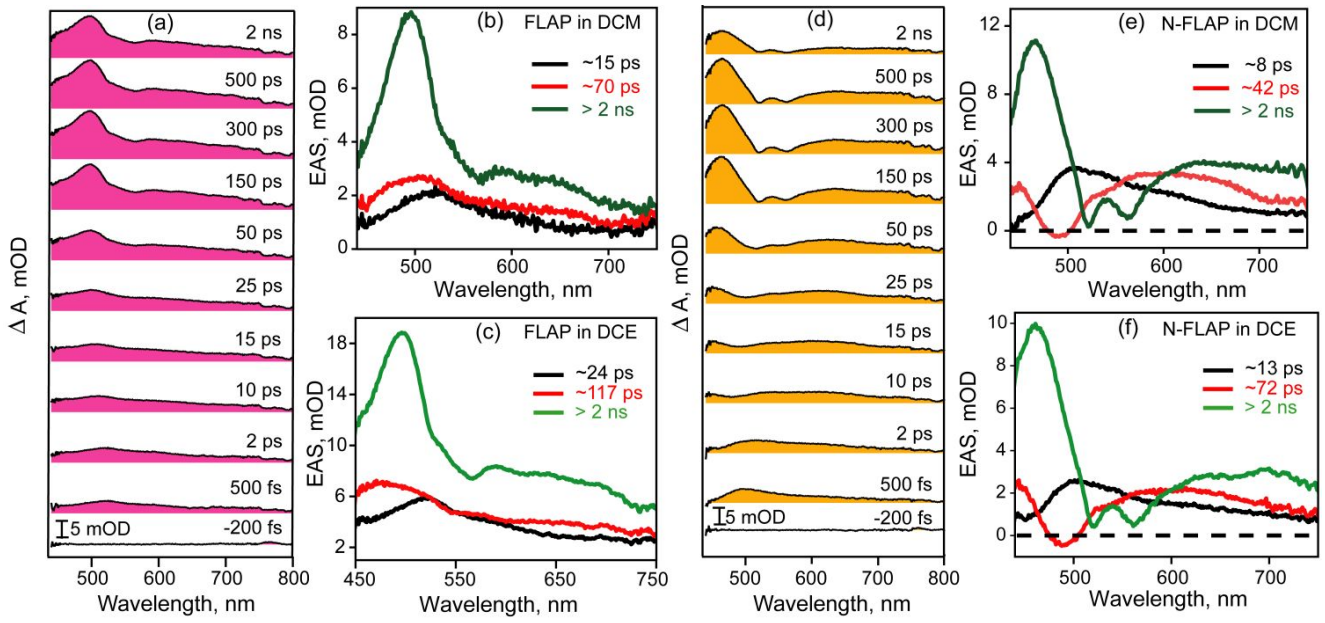

Figure 4. (a) Femtosecond transient absorption (TA) spectra at various time delays in the visible range for **FLAP** in DCM. The spectral traces are shown from 440 nm to 800 nm. Evolution associated spectra of the TA spectra obtained via singular value decomposition (SVD) are shown for (b) **FLAP** in DCM and (c) **FLAP** in DCE. (d) The corresponding spectra for **N-FLAP** in DCM. Evolution associated spectra of the TA spectra obtained via SVD are shown for (e) **N-FLAP** in DCM; and (f) **N-FLAP** in DCE.

shallow V-shaped geometry) observed in the TCSPC measurements. We ascertain the final state to be the planar emissive form of the molecule as the lifetime is >2 ns and is determined by the TCSPC measurements to be ~12 ns. On the other hand, the short 15 ps lifetime component was never observed in TCSPC measurements due to poor IRF of ~55 ps. Our computational investigation on the full **FLAP** geometry provided clear information on the vertical transitions associated with the V-shaped bent geometry. Firstly, the lowest singlet state geometry (S_0) was optimized using PBE0/6-31G(d) as shown in Figure S19 and S23. The calculated excitations at the TD-PBE0/6-31G(d) level suggested that the S_0 to S_1 transition in both **FLAP** and **N-FLAP** is symmetry forbidden while the transition to the closely located S_2 state (energy gap with 2.9613 eV) is dipole allowed for vertical excitation with substantial oscillator strength (Table S1 and S2). We therefore assign the initial excited state by the 400 nm pulsed light to be a bent S_2 state. The S_2 to S_1 internal conversion occurs in 15 ps which then leads to the emissive states; i.e. the slightly relaxed shallow V-shaped state and the fully relaxed planar state.

The optimized structures of **FLAP** in the S_2 and S_1 bent geometries (Figure S20a and S21) suggests a significant conformational change from a COT dihedral angle of ~142° in S_2 to ~159° in S_1. This opening up of the COT ring may result in the viscosity dependence of the S_2 lifetimes (see below).

We next probe the viscosity sensitivity of the lifetimes associated with the 3-state model by carrying out transient absorption measurements of **FLAP** in DCE. The spectral evolution after photoexcitation along with the evolution associated spectra (EAS) (in Figure 4c) and the associated lifetimes are obtained (Figure S5). On comparing the lifetimes in both the solvents (Figure S10), we observe a viscosity dependent decay of the initial S_2 state where the 15 ps lifetime in DCM is increased to 24 ps in DCE. Our data indicates a possible small geometry change within the 15 ps lifetime which therefore leads to the S_1 state through internal conversion. Lifetime of the bent emissive state is also enhanced from 70 ps to 117 ps hinting at a structural change associated with the decay of both the states.

Figure 4d shows the visible TA spectra of **N-FLAP** in DCM. In the spectral evolution, the locally excited absorption is seen initially in the 500 fs trace with an absorption maximum at ~500 nm (black trace with ~8 ps lifetime), which then gives rise to an absorption centered at 600 nm with a dip in the spectra at 480 nm (red trace with ~42 ps lifetime), possibly due to the convolution of stimulated emission from the slightly relaxed state. This state ultimately gives rise to the long-lived state with overlapping vibronic features of the stimulated emission from the relaxed planar emissive state (green trace with > 2ns lifetime), which the TCSPC reports as ~2.3 ns The depletion features on top of the excited state absorption (Figure 4e and f) comes at 490 nm in the initial S_2 state (red trace) which then red shifts to well resolved vibronic dips on the ESA (green trace). The vibronic features come at 520 and 560 nm which matched exactly with the steady state emission spectra vibronics (Figure 2) thereby indicating overlapping stimulated emission. This deconvoluted spectrum with the vibronic depletion features confirm the green spectra to come from the relaxed planar emissive state.

Femtosecond transient absorption studies in the NIR range: We found that transient absorption of **FLAP** and **N-FLAP** can be also observed in the NIR region. A similar 3-state evolution was obtained again, in which the lifetime of the first two states were viscosity dependent. For **FLAP** in DCM (Figure S4), the S_2 state has a lifetime of 19 ps followed by a 64 ps of the bent

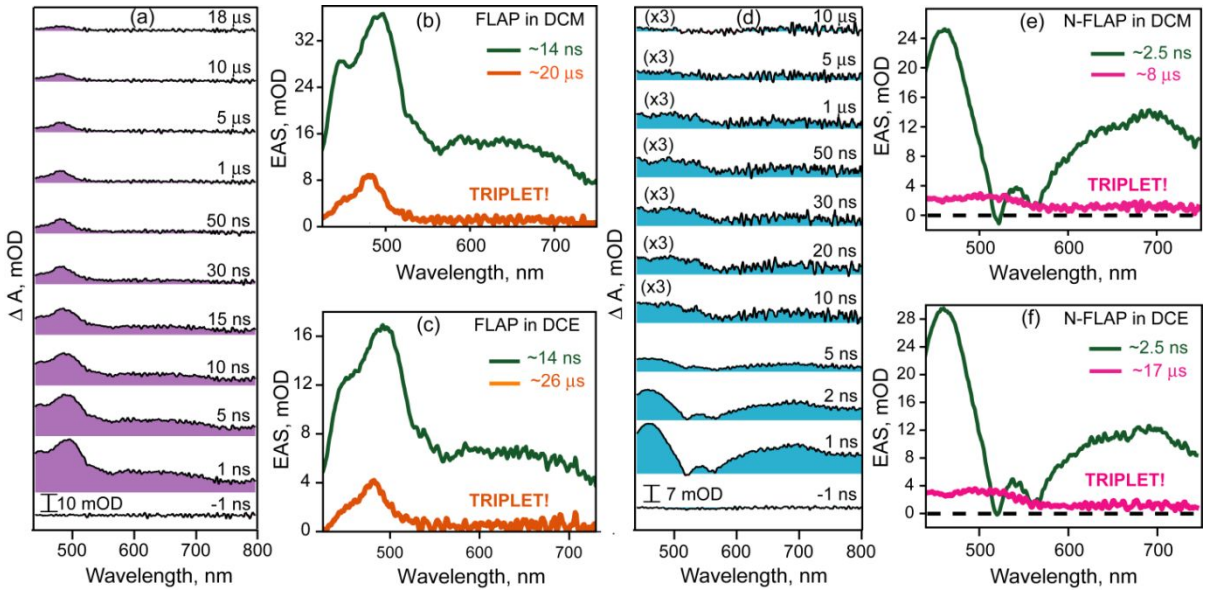

Figure 5. (a) Nano-to-microsecond TA spectra at various time delays for **FLAP** in DCM. Evolution associated spectra of the transient spectra obtained via SVD through a two-state sequential model are shown for (b) **FLAP** in DCM and (c) **FLAP** in DCE. (d) The corresponding spectra for **N-FLAP** in DCM. Evolution associated spectra of the TA spectra obtained via SVD are shown for (e) **N-FLAP** in DCM; and (f) **N-FLAP** in DCE.

emissive state. In the NIR range the lifetime of the S_2 state is slightly increased to 24 ps in DCE, and the shallow V-shaped emissive state had a lifetime of 110 ps (Figure S6). The >2 ns long-lived state in both visible and NIR transient absorption measurements did not have a viscosity dependent lifetime similar to what was also observed in TCSPC. Hence using both TCSPC and femtosecond broadband TA, we conclude that the decay of the S_2 state is concomitant with the rise of a shallow V-shaped emissive state which then evolves to a planar emissive state. DFT calculations previously conjectured[26] such planarization in the S_1 state, which we can now evidently characterize with their respective EAS spectra. Upon optimization of the full **FLAP** in S_1 state we obtained the S_1 planar structure at TD-PBE0/6-31G(d) level of theory (Figure S20b). We find that the S_1 minimum which shows a planar structure has ~180 degree dihedral angle which clearly enunciates the large structural motion of the wings to reach that planar geometry, and hence the viscosity dependence.

For **N-FLAP** in DCM, the NIR region (Figure S7) also shows a similar 3-state evolution with the lifetimes of 9 ps for locally excited state, 37 ps for the shallow V-shaped emissive and 2 ns for the relaxed planar emissive state. In DCE (Figure 4f), those lifetimes are prolonged to 13 ps (Figure S8 and S9), ~72 ps, and >2 ns (Figure S10), respectively. We note that in **N-FLAP** the locally excited state and the shallow V-shaped emissive state decay much faster than those in **FLAP** thereby hinting that planarization is more facile on the S_1 surface. A possible reason for this faster planarization could be because the S_1 surface in **N-FLAP** is predicted to have a smaller barrier and larger slope in the planarization coordinate[30].

Nano-to-microsecond transient absorption studies for triplet states: To observe the dynamics leading to triplet states, nano-to-microsecond transient absorption spectra were recorded in both DCM and DCE for **FLAP** and **N-FLAP** in inert condition. Figure 5a shows the excited state absorption within the visible range from 1 ns to 18 µs for **FLAP** in DCM. The initial 1 ns trace depicts the absorption spectra of the planar emissive state. There is a prominent change in the absorption spectra in the 30 ns trace with a blue shift in the absorption maximum which then decays away in few microseconds. Upon deconvolution, we observe a 14-ns state (green trace in Figure 5b), which matches with the TCSPC lifetime (~12 ns) depicting the planar emissive state. In addition, the planar emissive state also has an excited state absorption at ~952 nm in the NIR region which shows a mono-exponential decay of ~13 ns in both the solvents (Figure S12). This state drives the formation of the blue-shifted triplet state with peak at 482 nm and a lifetime of 20 µs in DCM (orange trace in Figure 5b). We checked the oxygen sensitivity to the triplet lifetime as shown in Figure 6a. We find that in ambient conditions (no degassing) the lifetime is evidently reduced to ~400 ns (red trace in Figure 6a) thereby confirming the triplet state assignment. This triplet spectrum is different from the triplet spectrum of a monomeric anthracene unit[39] (see Figure 6b).

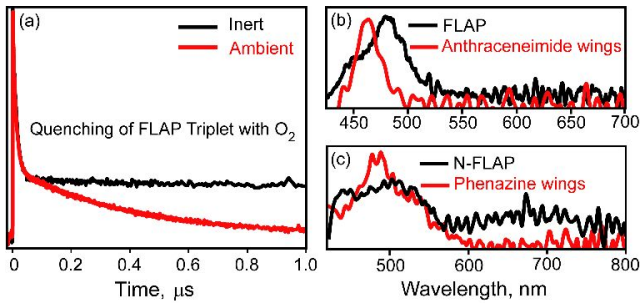

Figure 6: (a) Oxygen dependent triplet state quenching of **FLAP** in DCM. The kinetics is plotted at 482 nm subsequent to photoexcitation at 400 nm. The comparison of triplet absorption spectra in DCM at 50 ns for (b) anthraceneimide wing with **FLAP**; (c) phenazine wing with **N-FLAP**.

On comparing with the excited state dynamics in DCE (Figure 5c and S11), we see that the 14-ns lifetime of the planar emissive state remains intact. The result indicates no large amplitude structural change during the intersystem crossing (ISC) as well as the internal conversion. Therefore, the ISC to a triplet state is expected to proceed in a planar geometry. The triplet lifetime is slightly enhanced to 26 μs in DCE compared to the 20 μs observed in DCM although the spectral position remains unchanged (Figure S15 and S16). The origin of the viscosity dependent triplet lifetime has not been resolved.

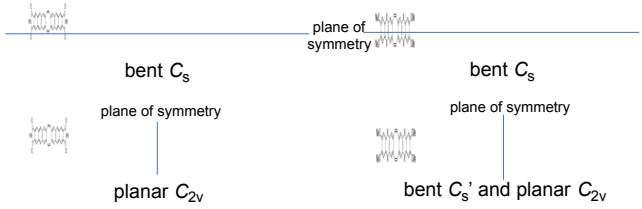

Figure 7. Structures of **FLAP′** (left) and **N-FLAP′** (right). In the optimized geometries with bent C_s symmetry in the triplet ground state, the two wings take asymmetric structures and the spin density is only delocalized over one wing (Figure S30, S34). On the other hand, in the optimized geometries with bent C_s' and planar C_{2v} symmetry, the C=C bond lengths of the *cis*-olefins in the COT ring are different (Figure S28, S32).

Figure 5d shows the ns–μs excited state absorption of **N-FLAP** in DCM. A triplet state was observed from the clear change in absorption from the 10-ns trace. The triplet nature of the long-lived state was confirmed from the oxygen dependence again (Figure S14). On deconvolution of the entire spectra, a 2.5 ns state (green trace in Figure 5e) was assigned to the planar emissive state due to the lifetime match with the TCSPC relaxed emission lifetime. Subsequently the triplet state forms as shown in the pink trace in Figure 5e having a lifetime of 8 μs. The spectrum of the **N-FLAP** triplet state is centered at ~500 nm with a much broader spectral width than that of **FLAP**. It should be noted that the isolated phenazine triplets provided a different spectral feature from that of **N-FLAP**[40] (see Figure 6c). The spectral shape and position of the triplet signature for **N-FLAP** reflects the electronic coupling of the two phenazine moieties in the molecule. The viscosity-independent lifetime of the emissive state was confirmed again, suggesting that the ISC occurs in a planar geometry of **N-FLAP**, very similar to that observed for FLAP. We also find that the lifetime of the emissive planar state decreases from 12 ns in **FLAP** to 2.5 ns in **N-FLAP** although the fluorescence quantum yields are comparable (Φ_F = 0.34 and 0.42, respectively). As a result, the radiative and nonradiative decay rates are estimated to be $k_r = 2.8 \times 10^7\ s^{-1}$ and $k_{nr} = 5.5 \times 10^7\ s^{-1}$ for **FLAP**, and $k_r = 16.8 \times 10^7\ s^{-1}$ and $k_{nr} = 23.2 \times 10^7\ s^{-1}$ for **N-FLAP**, respectively. It implies that the intersystem crossing rate of **N-FLAP** is much faster than that of **FLAP**. In absence of triplet sensitization experiments which need to be carefully carried out in future, we estimate that the triplet quantum yields cannot be greater than 58% for N-FLAP and 66% for FLAP.

DFT Structural optimization in the excited states: DFT calculations were performed for the study of the T_1 state. To reduce calculation costs, model structures **FLAP′** and **N-FLAP′** were calculated, which have hydrogen atoms and methyl groups in place of the 2,6-diisopropylphenyl groups of **FLAP** and the hexyl groups of **N-FLAP**, respectively (Figure 8, S27). Structural optimization in S_1 and T_1 was performed using the Gaussian 16 program (see the SI for the detail)[41]. All energy minimum structures have no imaginary frequency.

Firstly, energy diagrams of optimized geometries in T_1 were investigated for **FLAP′** and **N-FLAP′**. In constrained geometry optimization with fixed COT bending angles, the dihedral angle between C1-C2-C3 and C2-C3-C4 planes in Figure S27 was fixed. Structural optimization at each COT bending angle in the triplet ground state was firstly performed at UPBE0/6-31+G(d) levels of theory. In the structural optimization, three geometries at the (local) minima (planar C_{2v}, planar D_{2h}, and bent C_s) were found (Figure 7). In the T_1 optimization of the simplified chemical structures (**FLAP′** and **N-FLAP′**), the different geometries were obtained depending on the initial geometry. For instance, starting from the S_0 optimized V-shaped geometry, a shallow V-shaped saddle-point geometry with an imaginary vibration was obtained. After the displacement in the direction of the imaginary vibration, the planar C_{2v} geometry at the local minimum was obtained (Figure S28, S32). On the other hand, the planar D_{2h} geometry was obtained after symmetrizing the planar C_{2v} geometry and further optimization (Figure S29, S33). Finally, the bent C_s geometry was obtained, starting from an initial geometry that perturbed the C-C bond lengths of the central COT ring in the S_0 optimized V-shaped geometry (Figure S30, S34). The order of the energy levels of these three minima were the same in both **FLAP′** and **N-FLAP′**. The bent C_s geometry was most stable in T_1, while the planar D_{2h} was the least stable and the planar C_{2v} geometry lies between the other two minima. The energy gap increases with the percentage of Hartree-Fock exchange (HFX) due to the higher stabilization of planar structures by methods with a small amount of HFX (see Figure S31 and S34 for the detail)[42-44].

Aromaticity evaluation in S_1 and T_1: Ottosson and co-workers previously investigated the aromaticity of π-expanded COT systems, in which the original Baird aromaticity of the triplet COT was significantly reduced by the aromatic ring fusion[45]. We have computationally investigated the aromaticity indexes of **FLAP′** and **N-FLAP′** in T_1 with the planar C_{2v} symmetry. Here we selected PBE0 as a functional because, in many cases, PBE0 shows a good correspondence with experimental results of the **FLAP** system such as the absorption and fluorescence properties[46].The results were compared to those of the planar geometry in S_1, optimized at TD-PBE0/6-31+G(d) levels of theory (Figure S36)[38]. In S_1, while **FLAP′** took a planar C_{2v} geometry at the global minimum, **N-FLAP′** gave a planar D_{2h} geometry in this calculation level. Standard aromaticity indices in the magnetic criteria such as the nucleus-independent chemical shifts (NICS)[47] and the anisotropy of the induced current density (ACID)[48], the geometrical criteria such as the harmonic oscillator model of aromaticity (HOMA)[49] and the new HOMA for heterocycle electron delocalization (HOMHED),[50] and the electron-sharing criteria such as the aromatic fluctuation index (FLU)[51] and the multicenter index

(MCI)[52] were computed for the optimized geometries at the local minima in S_1 and T_1 with the planar geometries. To compare the degree of the aromaticity, we have also calculated the same indices of reference compounds in T_1, dibenzocyclooctatetraene (DBCOT in Figure S37; planar D_{2h})[45] and cyclooctatetraene (COT in Figure S38; planar D_{8h})[11], which have been reported to show Baird aromaticity in T_1. Besides, density functional approximations (DFAs) with a low percentage of HFX are expected to overstate aromaticity[42-44] and, therefore species characterized as non-aromatic by these methods will be also identified as such by DFAs with large amounts of HFX.

		FLAP′	N-FLAP′	DBCOT	COT
NICS(0)	T_1	+2.74	+2.35	–12.52	–11.11
NICS(1)	T_1	+0.90	+0.55	–12.01	–10.90
$NICS(1)_{zz}$	T_1	+6.32	+4.89	–33.54	–32.20
HOMA	S_1	0.49	0.41	0.62	0.94
	T_1	0.25	0.22	0.65	0.94
HOMHED	S_1	0.84	0.81	0.88	0.98
	T_1	0.76	0.76	0.89	0.98
FLU	S_1	0.015	0.016	0.012	0.000
	T_1	0.027	0.027	0.011	0.001
MCI	S_1	0.0025	0.0019	0.0034	0.0096
	T_1	0.0021	0.0023	0.0091	0.0289

Table 1. Aromaticity indices of the COT ring of **FLAP′** (planar C_{2v} for S_1 and T_1), **N-FLAP′** (planar D_{2h} for S_1 and planar C_{2v} for T_1), DBCOT (planar D_{2h} for S_1 and T_1), and COT (planar D_{8h} for T_1). HOMA and HOMHED values were obtained with the geometries optimized at the (U)PBE0/6-31+G(d) level. NICS, FLU and MCI values were calculated for those geometries at the (U)PBE0/6-31+G(d) level.

The values of those indexes at the central COT ring were summarized in Table 1. While all benzene and pyrazine rings of **FLAP′** and **N-FLAP′** in T_1 have negative NICS(0), NICS(1), and $NICS(1)_{zz}$ values, the COT ring has positive NICS values (for $NICS(1)_{zz}$, **FLAP′**: +6.32 ppm, **N-FLAP′**: +4.89 ppm) while the COT ring of DBCOT and COT have large negative NICS values in T_1 (DBCOT: –33.54 ppm, COT: –32.20 ppm; summarized in Figure S39). The nonaromatic character of the COT ring of **FLAP′** and **N-FLAP′** in T_1 was also confirmed by ACID calculation. No aromatic ring current including the COT ring was confirmed in **FLAP′** and **N-FLAP′** in T_1, although the aromatic ring current along the perimeter of DBCOT and COT were observed (Figure 8). In addition, HOMA at the COT ring in T_1 (**FLAP′**: 0.25, **N-FLAP′**: 0.22) are significantly lower than those of benzene and pyrazine rings (**FLAP′**: 0.47 to 0.69, **N-FLAP′**: 0.48 to 0.77). In S_1, those geometrical indexes of the COT rings (**FLAP′**: 0.49, **N-FLAP′**: 0.41) and the benzene and pyrazine rings (**FLAP′**: 0.59 to 0.66, **N-FLAP′**: 0.36 to 0.59) are not largely different (Figure S40). Those HOMA values of the COT ring are much lower than parent COT (S_1: 0.94, T_1: 0.94) and even significantly lower than those of DBCOT (S_1: 0.62, T_1: 0.65). HOMHED also indicated the similar tendency. Furthermore, higher FLU values and lower MCI values of the COT rings of **FLAP′** and **N-FLAP′** in T_1 (for FLU, **FLAP′**: 0.027, **N-FLAP′**: 0.027 and for MCI, **FLAP′**: 0.0021, **N-FLAP′**: 0.0023), compared to those of references in T_1 (for FLU, DBCOT: 0.011, COT: 0.001 and for MCI, DBCOT: 0.0091, COT: 0.0289), suggested that the aromaticity was practically lost by acene elongation (Figure S41, S42)[27,45]. Overall, these results indicated that the COT ring in the planarized T_1 geometries of **FLAP′** and **N-FLAP′** are not Baird aromatic.

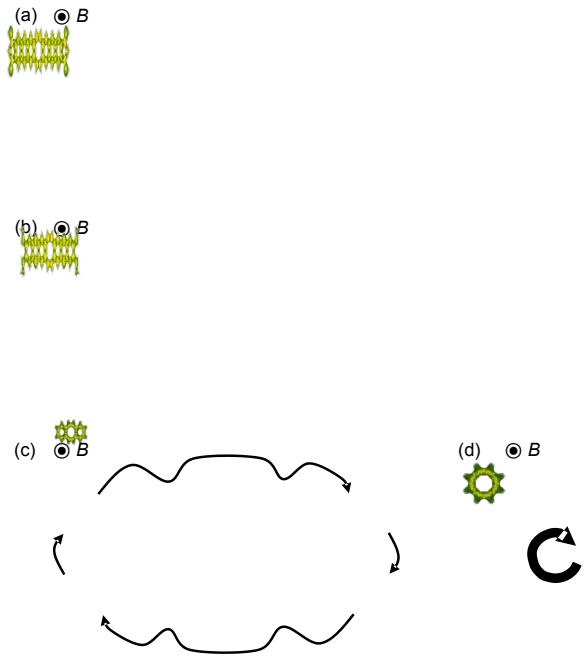

Figure 8. ACID plots for (a) **FLAP′** (planar C_{2v}), (b) **N-FLAP′** (planar C_{2v}), (c) DBCOT (planar D_{2h}), and (d) COT (planar D_{8h}) in T_1 at the UPBE0/6-31+G(d) level of theory. Current density isosurface at 0.05 au.

We hypothesize that the driving force for planarization in **FLAP** and **N-FLAP** is not Baird aromaticity[45], but rather excited state conjugation enhancement (ESCE)[53]. Baird aromaticity is only observed for smaller **FLAPs** bearing short π-conjugation[25,27]. In the case of Baird aromatic systems, clear stabilization energy (>10 kcal/mol) is expected by the S_1 planarization, and there should be a barrierless S_1 energy profile[54]. Therefore, the planarization dynamics is very fast, less than 1 ps. On the other hand, **FLAP** and **N-FLAP** switches the S_1 configuration during the planarization, giving a small energy barrier[27,28,30,38]. These molecules also show the excited-state planarization, but the dynamics is much slower than 1 ps. For example, the planarization dynamics of **FLAP** derivatives are reported to be 4 ps (CH_2Cl_2)[27] and 550 ps (DMSO)[26]. In addition, the stabilization energy due to ESCE is much smaller than 10 kcal/mol[27,28,30,38].

Discussion on the triplet conformation: While the DFT calculations predicted the bent conformations as the most stable triplet geometries for both **FLAP** and **N-FLAP**, the experimental studies do not necessarily indicate the formation of the bent triplet species. Triplet-triplet (TT) absorption spectra of these compounds were compared with those of the corresponding "wing" monomers, anthraceneimide and phenazine bearing the same substituents, at the 50 ns time

delay (Figure 6b and 6c). TT absorption spectrum of **FLAP** has a peak at 485 nm with a full width at half maximum (FWHM) of ~2640 cm^{-1} and a broad detectable feature at 600-800 nm, while that of anthraceneimide showed a peak at 463 nm with FWHM of ~1200 cm^{-1} and no feature was observed in the long-wavelength region (Figure 6b). The situation was also true for **N-FLAP** and the phenazine monomer (Figure 6c). It worth noting that calculated TT absorption patterns of planar C_{2v} **FLAP'** and **N-FLAP'** (Figures 9a and 9b, red) are clearly different from those of the wing monomers (Figures 9c and 9c, green), and bent C_s **FLAP'** and **N-FLAP'** (Figures 9a and 9b, blue) provide similar patterns to the monomers.These results suggest that the two wings are electronically coupled in the triplet form, rather than isolated. This delocalized nature is more consistent with those triplets in the planar geometries, rather than the bent geometries (see the SI). Such discrepancy between theory and experiments could be partially reduced by a more realistic simulation including solvent effects and employing multi-reference methods, which are beyond the scope of the current manuscript.

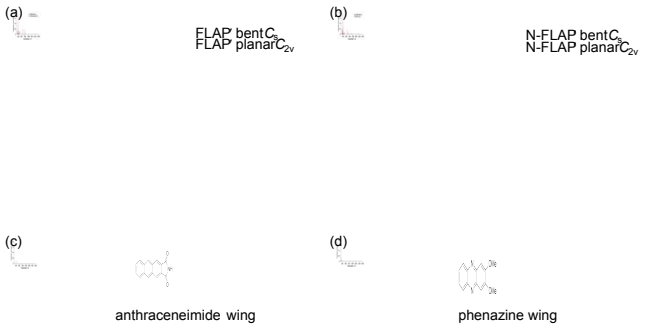

Figure 9. Calculated TT absorption patterns of (a) **FLAP'**, (b) **N-FLAP',** (c) anthraceneimide wing and (d) phenazine wing, calculated at the TD-UPBE0/6-31+G(d) level. Blue and red bars indicate oscillator strengths of **FLAP'** or **N-FLAP'** at the T_1 optimized bent C_s and planar C_{2v} geometries, respectively.

Conclusion

We report the optical signatures of the triplet states of COT-based flapping fluorophores for the first time by vertical photoexcitation on the fluorophores. We observed for both **FLAP** and **N-FLAP** that the intersystem crossing mechanism does not involve a discernable geometry change, and therefore assign a planar conformation for the COT backbone as the system reaches the T_1 surface. The long-lived and O_2 sensitive absorptions were confirmed with up to microsecond lifetime as the evidence for the generation of the triplet species. DFT calculations predicted the bent triplet geometry as most stable conformation, ruling out the aromaticity of the planar triplet geometries in the effectively π-expanded COT compounds. On the other hand, based on the experimental studies by the comparison of the flapping fluorophores and the corresponding wing monomers in the triplet-triplet absorption spectra, the assignment of electronically delocalized planar triplet geometries of **FLAP** and **N-FLAP** are rather consistent.

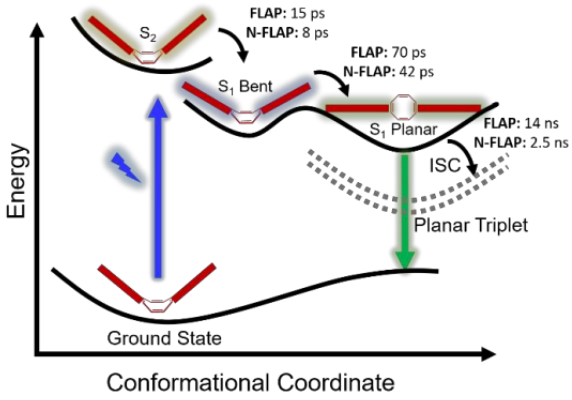

Figure 10. Potential energy surface rendition of the excited state evolution for **FLAP**/**N-FLAP** chromophores based on our steady-state and transient experiments described here. The initial bright S_2 state is formed upon photoexcitation which internally converts to the S_1 state having two conformations: shallow-V-shaped and planar. The bent-to-planar conformational change takes place in tens of picoseconds for both **FLAP** and **N-FLAP**. The planar S_1 then forms a planar triplet which then relaxes back to the bent form in the ground state. The time constants observed in the DCM solutions are demonstrated.

Overall, we suggest a generic mechanism for these flapping dyes which involves intersystem crossing concomitant with the radiative decay (the green emission) as demonstrated in Figure 10. From our experimental measurements, we report that the major structural evolution of these flapping dyes mostly take place on the singlet surfaces. In fact, a structural relaxation from S_2 to a shallow V-shaped emissive S_1 state is an initiating step for a subsequent larger amplitude motion needed to reach the planar conformation on the S_1 surface. The triplets evolve from the planar singlet state via an intersystem crossing process whose rates largely dictate the singlet lifetime.

In future a clear understanding of the planarization process on the singlet surface would be extracted using broadband vibrational spectroscopy. The interplay of certain low-frequency torsional modes in the COT backbone that drive the planarization process would be necessary to tune the planarization timescales.

ASSOCIATED CONTENT

Supporting Information. Description of the materials and experimental methods, additional figures pertaining to the experiments are given in the Supporting Information.

Corresponding Authors:

Jyotishman Dasgupta – Department of Chemical Sciences, Tata Institute of Fundamental Research, Mumbai 400005, India; orcid.org/0000-0003-4607-653X; Email: dasgupta@tifr.res.in

Shohei Saito - Department of Chemistry, Graduate School of Science, Kyoto University, Kyoto, Japan, Email: saito.shohei.4c@kyoto-u.ac.jp

Author Contributions J.D. conceived the research while S.P., S.S. and J.D. planned the initial experiments. R.K., H.K. and N.D. synthesized the molecules. S.P. performed the spectroscopy experiments and analyzed the experimental data with contributions from J.D. and S.S. The electronic structure

and aromaticity calculations were performed by H.K., K.S. and S.P. with inputs from R.V. and E.M. The manuscript was written by S.P. and J.D. with contributions from S.S., H.K., K.S., R.K. and R.V. All the co-authors discussed the scientific content in detail and agreed with the final form of the manuscript.

ACKNOWLEDGMENTS

S.P, R.V and J.D. acknowledge support from the Department of Atomic Energy (DAE), Government of India, under Project no. 12-R&D-TFR-5.10-0100. S.S, H.K., and K.S. thank the financial support from JST FOREST (JPMJFR201L), JSPS KAKENHI (JP21H01917), and JSPS Fellowships (JP22J21715). E.M. acknowledges financial support from the DIPC (DIPC_INV_003132). J.D. would like to thank Dr. Vamsee Voora (TIFR) for his very helpful comments with electronic structure calculations; and Mr. Mitradip Das (TIFR) for help with defining reaction coordinate for singlet state planarization. The authors gratefully acknowledge the discussion with Dr. Arup Kundu, Mr. Dipin Tomer, Mr. Debojyoti Roy, Mr. Kishan Yadav (TIFR Mumbai). The authors thank Ms. Mamta Kallianpur (TIFR Mumbai) for help in the TCSPC measurements.

References:

1 K. H. Claus, and C. Krüger, Structure of cyclooctatetraene at 129 K. *Acta Crystallographica Section C: Crystal Structure Communications* **1988**, 44, 1632-1634.
2 H. Kaufman, I. Fankuchen, and H. Mark, An X‐Ray Examination of Cyclooctatetraene. *The Journal of Chemical Physics* **1947**, 15, 414- 415.
3 Anet, F. A. L., The rate of bond change in cycloöctatetraene. *Journal of the American Chemical Society* **1962**, 84, 671-672.
4 E. Lippincott, R. Lord, and R. McDonald, The Vibrational Spectra and Structure of Cycloöctatetraene. *Journal of the American Chemical Society* **1951**, 73, 3370-3385.
5 J. Bordner, R. Parker, and R. Stanford, The crystal structure of octamethylcyclooctatetraene. *Acta Crystallographica Section B: Structural Crystallography and Crystal Chemistry* **1972**, 28, 1069- 1075.
6 P. G. Wenthold, D. A. Hrovat, W. T. Borden, and W. C. Lineberger, Transition-state spectroscopy of cyclooctatetraene. *Science* **1996**, 272, 1456-1459.
7 F. A. L. Anet, A. J. R. Bourn, and Y. S. Lin, Ring inversion and bond shift in cyclooctatetraene derivatives. *Journal of the American Chemical Society* **1964**, 86, 3576-3577.
8 D. A. Hrovat, and W. T. Borden, CASSCF calculations find that a D8h geometry is the transition state for double bond shifting in cyclooctatetraene. *Journal of the American Chemical Society* **1992**, 114 , 5879-5881.
9 J. L. Andrés, O. Castano, A. Morreale, R. Palmeiro, and R. Gomperts, Potential energy surface of cyclooctatetraene. *The Journal of chemical physics* **1998**, 108, 203-207.
10 M. J. Dewar, and K. M. Merz Jr, Potential energy surfaces and tunneling dynamics of some JahnTeller active molecules. *The Journal of Physical Chemistry* **1985**, 89, 4739-4744.
11 P. B. Karadakov, Aromaticity and antiaromaticity in the lowlying electronic states of cyclooctatetraene. *The Journal of Physical Chemistry A* **2008**, 112, 12707-12713.
12 N. C. Baird, Quantum organic photochemistry. II. Resonance and aromaticity in the lowest 3pp* state of cyclic hydrocarbons. *Journal of the American Chemical Society* **1972**, 94, 4941-4948.
13 N. Baird, Dewar resonance energy. *Journal of Chemical Education* **1971**, 48, 509.
14 L. Schaad, and B. A. Hess, Dewar resonance energy. *Chemical Reviews* **2001**, 101, 1465-1476.
15 Q. Zheng, S. Jockusch, G. G. Rodríguez-Calero, Z. Zhou, H. Zhao, R. B. Altman, H. D. Abruña, and S. C. Blanchard, Intramolecular triplet energy transfer is a general approach to improve organic fluorophore photostability. *Photochemical & Photobiological Sciences* **2016**, 15, 196-203.
16 S. Schols, A. Kadashchuk, P. Heremans, A. Helfer, and U. Scherf, Triplet excitation scavenging in films of conjugated polymers. *ChemPhysChem* **2009**, 10, 1071- 1076.
17 P. Tinnefeld, and T. Cordes, 'Selfhealing' dyes: intramolecular stabilization of organic fluorophores. *Nature Methods* **2012**, 9, 426-427.
18 R. B. Altman, D. S. Terry, Z. Zhou, Q. Zheng, P. Geggier, R. A. Kolster, Y. Zhao, J. A. Javitch, J. D. Warren, and S. C. Blanchard, Cyanine fluorophore derivatives with enhanced photostability. *Nature Methods* **2012**, 9, 68-71.
19 A. K. Pati, O. El Bakouri, S. Jockusch, Z. Zhou, R. B. Altman, G. A. Fitzgerald, W. B. Asher, D. S. Terry, A. Borgia, and M. D. Holsey, Tuning the Baird aromatic triplet-state energy of cyclooctatetraene to maximize the self-healing mechanism in organic fluorophores. *Proceedings of the National Academy of Sciences* **2020**, 117, 24305- 24315.
20 P. Forward, A. Gorman, and I. Hamblett, 'Nonvertical' triplet energy transfer to cyclooctatetraene: support for the singlebond torsion mechanism. *Journal of the Chemical Society, Chemical Communications* **1993**, 250-251.
21 L. M. Frutos, O. Castano, J. L. Andrés, M. Merchán, and A. U. Acuna, A theory of nonvertical triplet energy transfer in terms of accurate potential energy surfaces: The transfer reaction from π , π * triplet donors to 1,3,5,7-cyclooctatetraene. *The Journal of Chemical Physics* **2004**, 120, 1208- 1216.
22 L.-M. Frutos, O. Castano, and M. Merchán, Theoretical determination of the singlet→ singlet and singlet→ triplet electronic spectra, lowest ionization potentials, and electron affinity of cyclooctatetraene. *The Journal of Physical Chemistry A* **2003**, 107, 5472-5478.
23 B. Zietek, P. Targowski, A. Baczynski, and J. Bissinger, In Cyclooctatetraene as a triplet quencher in Dye lasers, Laser Technology II, *International Society for Optics and Photonics* **1987**, 25-29.
24 T. N. Das, and K. I. Priyadarsini, Triplet of cyclooctatetraene: Reactivity and properties. *Journal of the Chemical Society, Faraday Transactions* **1994**, 90, 963-968.
25 M. Hada, S. Saito, S. i. Tanaka, R. Sato, M. Yoshimura, K. Mouri, K. Matsuo, S. Yamaguchi, M. Hara, and Y. Hayashi, Structural monitoring of the onset of excited state aromaticity in a liquid crystal phase. *Journal of the American Chemical Society* **2017**, 139, 15792- 15800.
26 R. Kotani, H. Sotome, H. Okajima, S. Yokoyama, Y. Nakaike, A. Kashiwagi, C. Mori, Y. Nakada, S. Yamaguchi, A. Osuka, A. Sakamoto, H. Miyasaka and S. Saito, Flapping viscosity probe that shows polarity independent ratiometric fluorescence. *Journal of Materials Chemistry C* **2017**, 5, 5248-5256.
27 T. Yamakado, S. Takahashi, K. Watanabe, Y. Matsumoto, A. Osuka, and S. Saito, Conformational Planarization versus Singlet Fission: Distinct Excited‐State Dynamics of Cyclooctatetraene‐Fused Acene Dimers. *Angewandte Chemie International Edition* **2018**, 130, 5536-5541.
28 C. Yuan, S. Saito, C. Camacho, S. Irle, I. Hisaki, and S. Yamaguchi, A π -conjugated system with flexibility and rigidity that shows environment-dependent RGB luminescence. *Journal of the American Chemical Society* **2013**, 135, 8842-8845.
29 R. Kimura, H. Kitakado, T. Yamakado, H. Yoshida, and S. Saito, Probing a Microviscosity Change at the Nematic-

Isotropic Liquid Crystal Phase Transition by a Ratiometric Flapping Fluorophore. *Chemical Communications* **2022**, 58, 2128- 2131.

30 Y. Goto, S. Omagari, R. Sato, T. Yamakado, R. Achiwa, N. Dey, K. Suga, M. Vacha, and S. Saito, Dynamic Polymer Free Volume Monitored by Single-Molecule Spectroscopy of a Dual Fluorescent Flapping Dopant. *Journal of the American Chemical Society* **2021**, 143, 14306-14313.

31 H. Song, Y. Nam, D. Keefer, M. Garavelli, S. Mukamel, and S. Tretiak, Nonadiabatic Molecular Dynamics Study of the Relaxation Pathways of Photoexcited Cyclooctatetraene. *The Journal of Physical Chemistry Letters* **2021**, 12, 5716-5722.

32 M. Garavelli, F. Bernardi, A. Cembran, O. Castano, L. M. Frutos, M. Merchán, and M. Olivucci, Cyclooctatetraene computational photo-and thermal chemistry: A reactivity model for conjugated hydrocarbons. *Journal of the American Chemical Society* **2002**, 124, 13770-13789.

33 Y. Chen, S.-M. Tseng, K.- H. Chang, and P.-T. Chou, Energy Counterbalance to Harness Photoinduced Structural Planarization of Dibenzo[b,f]azepines toward Thermal Reversibility. *Journal of the American Chemical Society* **2022**, 144, 1748‑1757.

34 V. Balzani, F. Bolletta, and F. Scandola, Vertical and "nonvertical" energy transfer processes. A general classical treatment. *Journal of the American Chemical Society* **1980**, 102, 2152-2163.

35 A. A. Gorman, I. Hamblett, F. A. P. Rushton, and D. J. Unett, 'Nonvertical' triplet energy transfer to a severely non-planar 1,3-diene: proposal of a mechanism based on progressive endothermicity of vertical transfer to individual single-bond torsional levels. *Journal of the Chemical Society, Chemical Communications* **1993**, 983-984.

36 R. N. Jones, The ultraviolet absorption spectra of anthracene derivatives. *Chemical Reviews* **1947**, 41, 353-371.

37 O. Ryazanova, I. Voloshin, V. Makitruk, V. Zozulya, and V. Karachevtsev, pH-induced changes in electronic absorption and fluorescence spectra of phenazine derivatives. *Spectrochimica Acta Part A: Molecular and Biomolecular Spectroscopy* **2007**, 66, 849-859.

38 K. Suga, T. Yamakado, and S. Saito, Nitrogen-Substitution in the Flapping Wings of Cyclooctatetraene-Fused Molecules. *Bulletin of the Chemical Society of Japan* **2021**, 94, 1999-2002.

39 R. Compton, K. Grattan, and T. Morrow, Extinction coefficients and quantum yields for triplet–triplet absorption using laser flash photolysis. *Journal of Photochemistry* **1980**, 14 , 61-66.

40 T. G. Pavlopoulos, Triplet–triplet absorption and polarization spectra of phenazine. *Spectrochimica Acta Part A: Molecular Spectroscopy* **1987**, 43, 715-716.

41 M. J. Frisch, G. W. Trucks, H. B. Schlegel, G. E. Scuseria, M. A. Robb, J. R. Cheeseman, G. Scalmani, V. Barone, G. A. Petersson, H. Nakatsuji, X. Li, M. Caricato, A. V. Marenich, J. Bloino, B. G. Janesko, R. Gomperts, B. Mennucci, H. P. Hratchian, J. V. Ortiz, A. F. Izmaylov, J. L. Sonnenberg, D. Williams-Young, F. Ding, F. Lipparini, F. Egidi, J. Goings, B. Peng, A. Petrone, T. Henderson, D. Ranasinghe, V. G. Zakrzewski, J. Gao, N. Rega, G. Zheng, W. Liang, M. Hada, M. Ehara, K. Toyota, R. Fukuda, J. Hasegawa, M. Ishida, T. Nakajima, Y. Honda, O. Kitao, H. Nakai, T. Vreven, K. Throssell, J. A., Jr Montgomery, J. E. Peralta, F. Ogliaro, M. J. Bearpark, J. J. Heyd, E. N. Brothers, K. N. Kudin, V. N. Staroverov, T. A. Keith, R. Kobayashi, J. Normand, K. Raghavachari, A. P. Rendell, J. C. Burant, S. S. Iyengar, J. Tomasi, M. Cossi, J. M. Millam, M. Klene, C. Adamo, R. Cammi, J. W. Ochterski, R. L. Martin, K. Morokuma, O. Farkas, J. B. Foresman, and D. J. Fox, Gaussian 16, Revision A.03, *Gaussian*, Inc., Wallingford, **2016**.

42 I. Casademont-Reig, and R. GuerreroAvilés, E. Ramos-Cordoba, M. Torrent-Sucarrat, E. Matito, How Aromatic Are Molecular Nanorings? The Case of a SixPorphyrin Nanoring. *Angewandte Chemie International Edition* **2021**, 60, 24080‑24088.

43 I. Casademont-Reig, E. RamosCordoba, M. Torrent-Sucarrat, and E. Matito, How Do the Hückel and Baird Rules Fade Away in Annulenes? *Molecules* **2020**, 25, 711.

44 I. Casademont-Reig, T. Woller, J. Contreras-García, M. Alonso, M. Torrent-Sucarrat, and E. Matito, New Electron Delocalization Tools to Describe the Aromaticity in Porphyrinoids. *Physical Chemistry Chemical Physics* **2018**, 20, 2787‑2796.

45 R. Ayub, O. E. Bakouri, K. Jorner, M. Solà, and H. Ottosson, Can Baird's and Clar's Rules Combined Explain Triplet State Energies of Polycyclic Conjugated Hydrocarbons with Fused 4n π - and (4n + 2) π -Rings? *Journal of Organic Chemistry* **2017**, 82, 6327‑6340.

46 T. Yamakado, and S. Saito, Ratiometric Flapping Force Probe That Works in Polymer Gels. *Journal of the American Chemical Society* **2022**, 144, 2804‑2815.

47 H. Fallah-Bagher-Shaidaei, C. S. Wannere, C. Corminboeuf, R. Puchta, and P. v. R. Schleyer, Which NICS Aromaticity Index for Planar Pi Rings Is Best? *Organic Letters* **2006**, 8, 863‑866.

48 D. Geuenich, K. Hess, F. Köhler, and R. Herges, Anisotropy of the Induced Current Density (ACID), a General Method to Quantify and Visualize Electronic Delocalization. *Chemical Reviews* **2005**, 105, 3758‑3772.

49 T. M. Krygowski, H. Szatylowicz, O. A. Stasyuk, J. Dominikowska, and M. Palusiak, Aromaticity from the Viewpoint of Molecular Geometry: Application to Planar Systems. *Chemical Reviews* **2014**, 114, 6383‑6422.

50 C. P. Frizzo, and M. A. P. Martins, Aromaticity in Heterocycles: New HOMA Index Parametrization. *Structural Chemistry 2012*, 23 , 375‑380.

51 E. Matito, M. Duran, and M. Solà, The Aromatic Fluctuation Index (FLU): A New Aromaticity Index Based on Electron Delocalization. *Journal of Chemical Physics* **2005**, 122, 14109.

52 P. Bultinck, R. Ponec, and S. Van Damme, Multicenter Bond Indices as a New Measure of Aromaticity in Polycyclic Aromatic Hydrocarbons. *Journal of Physical Organic Chemistry* **2005**, 18, 706‑718.

53 S. K. Behera, S. Y. Park, and J. Gierschner, Dual emission: classes, mechanisms, and conditions. *Angewandte Chemie International Edition* **2021**, 60, 22624-22638.

54 R. Kotani, L. Liu, P. Kumar, H. Kuramochi, T. Tahara, P. Liu, A. Osuka, P. B. Karadakov, and S. Saito, Controlling the S1 energy profile by tuning excited-state aromaticity. *Journal of the American Chemical Society* **2020**, 142, 14985-14992.